THE JOURNAL OF BIOLOGICAL CHEMISTRY
Vol. 279, No. 13, Issue of March 26, pp. 13035–13043, 2004

Printed in U.S.A.

A Natural Prothrombin Mutant Reveals an Unexpected Influence of A-chain Structure on the Activity of Human α-Thrombin*

Received for publication, November 13, 2003, and in revised form, January 9, 2004
Published, JBC Papers in Press, January 13, 2004, DOI 10.1074/jbc.M312430200

Raimondo De Cristofaro‡§¶, Sepideh Akhavan¶‖, Cosimo Altomare‡‡, Andrea Carotti‡‡, Flora Peyvandi‖, and Pier Mannuccio Mannucci‖**

*From the ‡Hemostasis Research Centre, Institute of Internal Medicine and Geriatrics, Catholic University School of Medicine, 00168 Rome, Italy, ‖Angelo Bianchi Bonomi Hemophilia and Thrombosis Center, and Fondazione Luigi Villa, IRCCS Maggiore Hospital University of Milan, 20121 Milan, Italy, the ‡‡Department of Pharmaceutical Chemistry, University of Bari, 70125 Bari, Italy, and **INSERM E0348, Faculté Xavier Bichat, University Paris 7, 75870 Paris, France*

We have recently identified in two unrelated patients with bleeding tendency a homozygous mutation causing a deletion of one of the two contiguous Lys^{9}/Lys^{10} residues in the A-chain of α-thrombin (ΔK9). We used *in vitro* expression analysis to clarify the role of the deletion of Lys^{9} or Lys^{10} in the thrombin function. The k_{cat}/K_m value of the hydrolysis by ΔK9 of the synthetic substrate Phe-Pip-Arg-*p*-nitroanilide (where Pip represents L-pipecolyl) and fibrinopeptide A was 18- and 60-fold lower, respectively, compared with wild type (WT). Interaction with antithrombin was also reduced in the mutant, the association rate being about 20-fold lower than in the WT thrombin. The sensitivity to sodium ion of ΔK9 was found significantly attenuated compared with the WT form. ΔK9 has a very weak platelet-activating capacity, attributed to a severely defective PAR1 interaction, whereas the binding to the platelet glycoprotein Ibα was unaffected. Likewise, the interaction with protein C was severely impaired, whereas interaction with thrombomodulin had a normal K_d value. At variance with these findings, both low affinity (basic pancreatic trypsin inhibitor) and high affinity (*N*-α-[2-naphthylsulfonyl-glycyl]-4-amidinophenylalanine-piperidide) thrombin inhibitors displayed a better binding to ΔK9 than to the WT form, indicating a better accommodation of these inhibitors into the catalytic pocket of ΔK9. A molecular dynamics simulation of the ΔK9 thrombin in full explicit water solvent provided support to the role of the A-chain in affecting conformation and catalytic properties of the B-chain, especially in some insertion loops of the enzyme, such as the 60-loop, as well as in the geometry of the catalytic triad residues.

Recently, a homozygous deletion mutation of one of the two contiguous Lys^{9}/Lys^{10} residues[1] in the A-chain of α-thrombin was identified in two unrelated Iranian patients with severe prothrombin deficiency and hemorrhagic diathesis (1). The level of prothrombin antigen measured in plasma was 15%, whereas the coagulant activity ranged from less than 1% to about 2.5% (1). Prothrombin deficiency is an autosomal recessive bleeding disorder characterized by two phenotypes: hypoprothrombinemia, with concomitantly low levels of coagulant activity and antigen (type I), and dysprothrombinemia, with very low activity but subnormal or normal antigen levels (type II). These disorders are rare, and there is always residual prothrombin procoagulant activity measurable in patients, the phenotype found in prothrombin-deficient mice indicating that complete prothrombin deficiency may be lethal in humans (2, 3). To date, 38 defects in the prothrombin gene have been identified in patients with dysprothrombinemia or hypoprothrombinemia (1, 4–7). Among these natural dysprothrombins, amino acid residues of the thrombin A-chain were found to be rarely involved (1, 4–7).

The A-chain in human thrombin is composed of 36 amino acid residues, which are connected to the catalytic B-chain by a single disulfide bond (8). This chain has no analog in the prototypic serine protease trypsin, although chymotrypsin and other trypsin-like blood coagulation enzymes, such as factor IX and factor XI, contain A-chain analogs (9, 10). Some structural analogies between the A-chains present in different serine proteases, as in the case of thrombin and chymotrypsin, were identified, although the function of the A-chain has not yet been well established.

The thrombin A-chain is organized mainly in a multiple-turn and partly helical conformation and a boomerang-like shape, making a smooth contour of the B-chain part, opposite to the active site pocket (8). The A-chain is topologically similar to the activation peptide of chymotrypsin(ogen) and connected in a similar manner through the Cys^{1}–Cys^{122} disulfide bridge to the B-chain. Most of the A-B chain interactions involve charged side chains; six are buried salt bridges, and 10 are involved in interchain hydrogen bonds (8). Stabilization within the A-chain also occurs, mostly via polar and salt bridge interactions. The N-terminal segment of the A-chain up to E1c is characterized by relatively weak electron density in the D-Phe-Pro-Arg-methyl ketone-thrombin crystal (8), and seems to have a high degree of conformational flexibility (8). The C-terminal segment up to Y14j is an amphiphilic α-helix forming one and one-half turns and showing a high degree of flexibility as well (8). The central region is the most rigid segment of the A-chain and contains strong salt bridges, such as that involving the Asp^{1a}–Lys^{9} side chains (8), which is characterized by a high electrostatic energy (−1.8 kcal/mol), significantly contributing to confer the boomerang-like shape to the chain (8).

Not all of the coagulation serine proteases bear an A-chain,

* This work was supported by the Italian Ministry of University and Research (MIUR, COFIN-2003). The costs of publication of this article were defrayed in part by the payment of page charges. This article must therefore be hereby marked "*advertisement*" in accordance with 18 U.S.C. Section 1734 solely to indicate this fact.

§ To whom correspondence should be addressed: Hemostasis Research Center, Institute of Internal Medicine, Catholic University School of Medicine, Largo F. Vito, 1, 00168 Rome, Italy. Tel.: 39-06-30154438; Fax: 39-06-30155915; E-mail: rdecristofaro@rm.unicatt.it.

¶ These authors contributed equally to this work

[1] The thrombin amino acid residues are numbered by the chymotrypsin(ogen) numbering system.

hence its general role has not been precisely established. In a previous study, carried out on bovine thrombin, it has been proposed that the A-chain, although strongly linked to the B-chain through strong electrostatic and apolar bonds, does not play a major role in the specificity of the enzyme catalytic activity (11). In contrast, subsequent studies carried out on human thrombin showed that isolated B-chain has a markedly reduced proteolytic and amidase activity compared with the native enzyme (12).

With the aim of gaining insights into the role of the A-chain in human thrombin, we used *in vitro* expression analysis of the natural mutant bearing a deletion of Lys^9 (ΔK9). The wild-type (WT)[2] prothrombin and mutant cDNAs were stably transfected in Chinese hamster ovary cell lines expressing high levels of prothrombin for experiments probing their functional properties. In order to understand their different functional properties, we performed a molecular dynamics (MD) simulation of the ΔK9 thrombin mutant in full explicit water solvent. Our simulation, in conjunction with a comparative analysis of available crystal structures of free or ligand-bound WT thrombins, provided insightful support to the role of the A-chain in affecting conformation and catalytic properties of the B-chain.

EXPERIMENTAL PROCEDURES

Patients—We investigated the molecular defects in two Iranian patients with prothrombin deficiency and a severe hemorrhagic diathesis. Clinical and laboratory findings pertaining to these patients were previously reported in detail (1).

DNA Analysis—Following DNA extraction from leukocytes, the coding region, intron/exon boundaries, and 5′- and 3′-untranslated regions of the prothrombin gene were amplified by PCR screened for mutations by single strand conformation polymorphism analysis and sequenced using an ABI PRISM BigDye Terminator Cycle Sequencing Kit (ABI 373; PerkinElmer Life Sciences). The primers used in the PCR and sequencing are identical to those used in a previous study (1).

Site-directed Mutagenesis and Construction of Expression Vectors—Full-length cDNA of human prothrombin (including 38 bp of 5′-untranslated region and 97 bp of 3′-untranslated region) was obtained by PCR amplification of M13mp18 (kindly provided by Dr. Barbara C. Furie). The construction of plasmid $PT7^{SalI}$ FII-WT^{EcoRI} was previously described (13).

To investigate the influence of the Lys^9 deletion (ΔK9) on prothrombin activity, mutant FII-ΔK9 was obtained by site-directed mutagenesis of PT7-^{SalI}FII-WT^{EcoRI} using a commercially available kit (Clontech, Palo Alto, CA). Oligonucleotide (5′-CTGTTCGA---GAAGTCGCTGGAGGACAAAACCGAAAGAGAGCTTCTAGAATCCTACATC-3′) spanning nucleotides 1021–1080 of the human FII cDNA were used to introduce an in-frame deletion of 3 bp, nucleotides 1029–1031 (GAA deletion). This primer also introduced a XbaI restriction site (underlined), arising from two silent CCT to TCT and GGA to AGA mutations at nucleotides 1065 and 1068, respectively, to facilitate screening for clones carrying the mutation. The cloned insert was sequenced, and sequencing confirmed that the mutation had been introduced.

To obtain stable cell lines expressing recombinant FII-WT and FII-ΔK9, we used dihydrofolate reductase-deficient Chinese ovary cells (CHO-DUKX-B11). These cells were grown in α-modified essential medium supplemented with 10% fetal bovine serum, 2 mmol/liter L-glutamine, 10 mmol/liter HEPES, pH 7.2, 100 units/ml penicillin G, 100 μg/ml streptomycin, and 8 μg/ml vitamin K1 (Phytonadione; Abbott), 10 μg/ml adenosine, 10 μg/ml deoxyadenosine, and 10 μg/ml thymidine in a 5% CO_2 atmosphere at 37 °C. The DNA of pED-FII-WT or pED-FII-ΔK301 (30 ng) were transfected by electroporation into 5×10^6 CHO cells according to the manufacturer's instructions. Two days after transfection, cells were selected for dihydrofolate reductase expression using medium deficient in ribonucleosides and deoxyribonucleotides. A single clone stably transfected with each construct and expressing high levels of FII was selected for further experiments.

Purification of Wild Type and ΔK9 Prothrombin—Activation of ΔK9 prothrombin was obtained using the Taipan snake venom, whereas ecarin slowly activated the mutant zymogen (data not shown). It is known that the Taipan snake prothrombin activator acts as a Factor Xa-Factor Va complex, since it directly activates prothrombin through cleavages of the Arg^{271}-Thr^{272} peptide bond at the junction between A-chain and fragment 2 besides the additional cleavage of the Arg^{320}-Ile^{321} peptide bond (14). Prothrombin activation was obtained by incubating for 2 h at 37 °C 1 μM ΔK9 prothrombin (or the WT form) with 0.2 mg/ml Taipan snake venom in 50 mM Tris-HCl, 150 mM NaCl, 2 mM $CaCl_2$, synthetic phospholipid reagent containing a colloidal silica activator and used at a 1:5 dilution of the stock solution (SynthAsil APTT reagent, Instrumentation Laboratory, Milan, Italy), pH 8.00. The generated active ΔK9 thrombin was successfully purified by cation exchange HPLC, being eluted ~5 min before WT thrombin. This finding is in agreement with the lack of one positive charge related to the missing lysine residue in the A-chain of the mutant thrombin. SDS-PAGE of pooled chromatographic peaks was carried out on 4–20% gradient gels under both reducing (5% β-mercaptoethanol) and nonreducing conditions in a Bio-Rad mini-PROTEAN II apparatus. The pooled peak contained a single band of roughly 36 kDa, whose identity was further checked by N-terminal sequencing. To obtain purified A-chain from both WT and ΔK9 thrombin, the peak obtained in the ion exchange chromatography was reduced by 5% β-mercaptoethanol and analyzed through RP-HPLC using a C4 resin (High Pore RP-304 250 × 4.6 mm; Bio-Rad). The applied gradient was 10–40% acetonitrile in 0.1% trifluoroacetic acid at a flow rate of 1.0 ml/min. The elution was followed at 224 nm. The peak relative to the A-chain was eluted after 17.8 min for the WT species, whereas it appeared after 17 min in the case of ΔK9 thrombin. These peaks were pooled, dried, and solubilized in acetonitrile/water/trifluoroacetic acid (49:49:2 by volume) before sequencing was performed. An automatic liquid phase sequencer (ABI-PerkinElmer model 477A) connected to an HPLC apparatus (ABI-PerkinElmer model 120A, PTH-analyzer), and a Bio-Rad reverse-phase C18 column were used to determine the N-terminal sequencing. Identification of the cleavage products was based on the amino acid sequences of the human prothrombin (15).

The concentration of recombinant thrombins was measured spectrophotometrically at 280 nm, using an extinction coefficient (0.1%) equal to 1.83. Active site titration was carried out spectrophotometrically, as previously reported (16). The purified enzyme was immediately aliquoted and frozen at −80 °C until use.

Effect of Na^+ and Viscosity on the Michaelis-Menten Parameters Pertaining to Hydrolysis of the Synthetic Substrates D-Phe-Pip-Arg-pNA—Michaelis-Menten parameters, k_{cat} and K_m, were calculated as previously detailed (16), in 10 mM Tris-HCl, 0.15 M NaCl, 0.1% polyethylene glycol 6000, pH 8.00, at 25 °C (buffer A). The enzyme concentration was typically 0.5 nM for WT and 5–10 nM for the ΔK9 thrombin form. In the experiments without sodium, NaCl was substituted with a cation not interacting with thrombin, tetramethylammonium chloride, which was used at the same concentration to keep constant the ionic strength of the solution (17).

The effect of the viscogenic agent sucrose, used over a 0–0.8 M concentration range in buffer A, was investigated according to a previously detailed kinetic and analytical scheme (16–19). Accordingly, the canonical scheme for serine proteases amidase activity was applied,

$$E + S \underset{k_{-1}}{\overset{k_{+1}}{\rightleftharpoons}} ES \xrightarrow{k_2} EP^* \xrightarrow{k_3} E + P$$

SCHEME 1

where k_{+1}, k_{-1}, k_2, and k_3 are the kinetic rate constant of the substrate association and dissociation, acylation, and deacylation of thrombin, respectively, and EP^* is the acyl-enzyme intermediate, and P is the final product. The equilibrium dissociation constant, K_d, can be calculated from the k_{-1}/k_{+1} ratio. Experimental data sets were simultaneously fitted to the appropriate equations (16, 17), using the GRAFIT software (Erithacus Software Ltd., Staines, UK).

Fibrinopeptide A Release—Fibrinopeptide A release by both WT and ΔK9 thrombin in buffer A was monitored by reverse transcriptase-HPLC, using a previously reported method (20). Purified plasmin- and fibronectin-free fibrinogen from American Diagnostica (Instrumentation Laboratory, Milan, Italy) was used as substrate. The enzyme concentration was 0.2 and 2 nM, for the WT and the mutated form, respectively. The Michaelis parameters were computed as indicated above for the synthetic substrate.

[2] The abbreviations used are: WT, wild type; AT, antithrombin; BPTI, basic pancreatic trypsin inhibitor; α-NAPAP, *N*-α-[2-naphthylsulfonylglycyl]-4-amidinophenylalanine-piperidide; MD, molecular dynamics; HPLC, high pressure liquid chromatography; *p*NA, *p*-nitroanilide; Pip, L-pipecolyl.

Measurement of k_{cat}/K_m for Protein C Activation and Interaction with Thrombomodulin—Hydrolysis by WT and ΔK9 thrombin of zymogen protein C, purchased from American Diagnostica (Instrumentation Laboratory, Milan, Italy), was performed in buffer A, as previously reported in detail (21). Hydrolysis of protein C (2 μM) was followed in the presence of 100 nM human thrombomodulin (American Diagnostica), since in the absence of the cofactor, the reaction was too slow to be correctly analyzed. Likewise, binding of the thrombin forms to immobilized human thrombomodulin (nonlipidated form, from American Diagnostica) was investigated according to a previously reported method (21).

Inhibition of WT and ΔK9 Thrombin Forms by Antithrombin, Bovine Pancreatic Trypsin Inhibitor (BPTI), and N-α-[2-Naphthylsulfonyl-glycyl]-4-amidinophenylalanine-piperidide (α-NAPAP)—Pseudo-first order kinetics formalism was used to investigate the interaction of WT and ΔK9 thrombin forms with antithrombin (AT) (Enzyme Research, Indianapolis, IN) in the absence and presence of heparin in buffer A. In the absence of heparin, AT was used in concentrations ranging between 10 and 15 μM in buffer A at 25 °C. The reaction with thrombin was started by adding 0.1 nM WT or 5–10 nM ΔK9, and the release of *p*-nitroaniline was measured as a function of time at 405 nm. The measurements were performed in duplicate. The association second order rate constant, k_{on}, for thrombin-AT interaction was calculated as reported (22). Progress curve kinetics was also used to derive the k_{on} value of AT interaction with WT and ΔK9 mutant thrombin in the presence of high molecular weight heparin from porcine intestinal mucosa (Sigma; sodium salt Grade I-A, 170 United States Pharmacopeia/mg, average M_r = 16,500), as described (22). Heparin concentration was equal to 75 nM in functional experiments using 0.15 μM AT, 0.15 nM WT form, or 10 nM ΔK9 and 100 μM Phe-Pip-Arg-*p*NA as the substrate.

WT and ΔK9 mutant thrombin interaction with BPTI (Sigma) was performed in buffer A, according to a previously described "matrix" method (21). Competitive inhibition of the synthetic substrate Phe-Pip-Arg-*p*NA hydrolysis was used to monitor the inhibitor interaction with both the WT and ΔK9 thrombins. BPTI effect on the substrate's hydrolysis was investigated using the inhibitor over a concentration range from 0 to 1 mM, whereas α-NAPAP (Sigma) was used between 0 and 100 nM concentration. All of the experimental points taken at different inhibitor concentrations (BPTI or α-NAPAP) as a function of the substrate concentration were simultaneously fitted to a competitive inhibition of the Michaelis equation, as previously reported (19), using the GRAFIT software (Erithacus Software). This method allowed us to calculate the equilibrium dissociation constant of the inhibitor's binding to thrombin.

Measurement of the PAR1 Peptide Hydrolysis—Hydrolysis of the PAR1 peptide (PAR1P, NH_2-LDPRSFLLRNPNDKYEPFWEDEE-COOH, synthesized by Primm s.r.l., Milan, Italy) by the different thrombin forms was followed by measuring the release of the peptide LDPR, resulting from the cleavage of the NH_2 terminus of PAR1, according to a previously described method (22). Briefly, 0.5 μM PAR1P peptide was incubated with 50–100 pM WT or 10 nM ΔK9 thrombins in 10 mM HEPES, 0.15 M NaCl, 0.1% polyethylene glycol 6000, pH 7.5, at 25 °C. At time intervals (1, 2, 3, 4, 8, 12, and 15 min), the reaction was stopped with 0.3 M $HClO_4$, and the cleaved peptide was measured by reversed-phase HPLC, using a 250 × 4.6-mm RP-304 column (Bio-Rad), as previously reported (22).

Interactions with Platelets—We compared the effects of WT and ΔK9 thrombins on the enzyme capacity to activate gel-filtered platelets, which were prepared in 10 mM Hepes, 0.15 M NaCl, 5.5 mM glucose, 0.2% bovine serum albumin, pH 7.50, at 25 °C, according to a previously described method (22). In these experiments, thrombin concentrations ranged from 0.5 to 128 nM. Aggregation of gel-filtered platelets ($3 \times 10^5/\mu l$) was studied in a PACKS 4 aggregometer (Helena Laboratories, Milan, Italy), using a final volume of 500 μl. Aggregation response was evaluated by taking into account the maximum velocity of transmittance increase per minute (expressed as a percentage of transmittance, set by using plain buffer).

Molecular Dynamics Calculations—The x-ray structure of human thrombin covalently bound to D-Phe-Pro-Arg-methyl ketone, determined at 1.9-Å resolution (Protein Data Bank entry 1ppb) (8), was used as the starting structure. The covalently bound inhibitor was removed, and the structure of the free enzyme was used as a template for generating the ΔK9 mutant protein (Swiss-Prot; available on the World Wide Web at www.expasy.ch). The protein structure was solvated with water in a periodic truncated octahedron, to produce a 12-Å water shell. All solvent molecules within 1.5 Å of any protein atom were then removed. The GROMACS 3.1.4-1 software package, running on a Linux PC cluster, was used for the MD simulations and analysis of the trajectories. The total charge of the ΔK9 protein was +2, and no counterions was added. The entire system consisted of 3060 protein atoms and 12,759 water molecules.

The initial structure ΔK9 mutant thrombin was energy-minimized by using 200 steps of steepest descent with the protein constrained and then 1000 steps of conjugate gradient, with the entire system free, in order to remove bad contacts. During the simulations, the system was coupled to an external temperature bath with a coupling constants of 0.1 ps (23). The Gromos-96 force field (24) was used for minimization procedures, with a time step of 2 fs. Water molecules were modeled according to the "simple point charge" model (25). The LINCS algorithm (26) was used to constrain all bond lengths. The nonbonded interactions were cut off at 8 Å (short range cut-off radius) and 12 Å (long range cut-off radius) for both Coulombic and Lennard-Jones interactions. The short range nonbonded interactions were updated every time step, whereas the interactions within the long range radius were updated every five time steps. Initial velocities were assigned according to a Maxwellian distribution at the desired temperature. The density of the system was adjusted by performing the first equilibration runs under number pressure temperature conditions by weak coupling to a bath of constant pressure (p = 1 bar, coupling time of 0.5 ps). The simulation, starting from the initial structure, was equilibrated by 50 ps of MD run with position restraints on the protein to allow the solvent molecules to be relaxed, followed by another 50-ps run without restraints. Production dynamics were performed under number volume temperature conditions for 18 ns, and the coordinates saved every 10 ps.

RESULTS AND DISCUSSION

Expression Study

To investigate the influence of the Lys^9 deletion on prothrombin biosynthesis, transient transfections were performed in COS-7 cells using the dicistronic pED vectors containing either FII-WT or FII-ΔK9 cDNAs. Enzyme immunoassay demonstrated that, compared with FII-WT, the prothrombin antigen level of FII-ΔK9 was 20% in conditioned media (similar to that observed on the patient's plasma) and 14% in cell lysates. Purification of the mutant active thrombin by ion exchange HPLC was effective as demonstrated by SDS-PAGE (see Fig. 1), showing a single band with an apparent molecular mass of about 36 kDa (see Fig. 1). The identity of the purified ΔK9 protein was checked by N-terminal sequencing of the A-chain, which showed the presence in both the mutant and the WT enzyme of the TFGSGE sequence, which corresponds to the segment generated upon cleavage of the prothrombin Arg^{284}-Thr^{285} peptide bond. This N-terminal sequence is autocatalytically produced by meizothrombin, which releases a N-terminal 13-mer peptide from the A-chain (27, 28). It is noteworthy that a long incubation time was indeed necessary to obtain a full ΔK9 prothrombin activation by Taipan snake venom, at variance with WT-FII, which under the same experimental conditions was almost fully activated after a 20-min incubation with Taipan venom (data not shown).

Hydrolysis of the Synthetic Substrate Phe-Pip-Arg-pNA: Effects of Na^+ and Viscosity

The effect on thrombin functions by Na^+ binding to the 225-loop, which triggers the transition of the enzyme from a slow form to a more active (fast) form, has been well established (29). Under the experimental conditions of this study, the best fit k_{cat} and K_m values for the WT form were equal to 88.9 ± 1.5 s^{-1} and 1.90 ± 0.13 μM in the Na^+-bound (fast) form, compared with 35.8 ± 1.2 s^{-1} and 9.98 ± 0.84 μM in the Na^+-free (slow) form. The same kinetic parameters in the ΔK9 thrombin were equal to 4.1 ± 0.2 s^{-1} and 1.6 ± 0.2 μM in the fast form, compared with 3.0 ± 0.3 s^{-1} and 5.1 ± 0.14 μM in the slow form. If the ratio between the k_{cat}/K_m values between the fast and the slow form is defined as r, then an energetic contribution (ΔG_c, kcal/mol) associated to such a functional transition can be calculated. Accordingly, $\Delta G_c = RT \ln r$, where R is

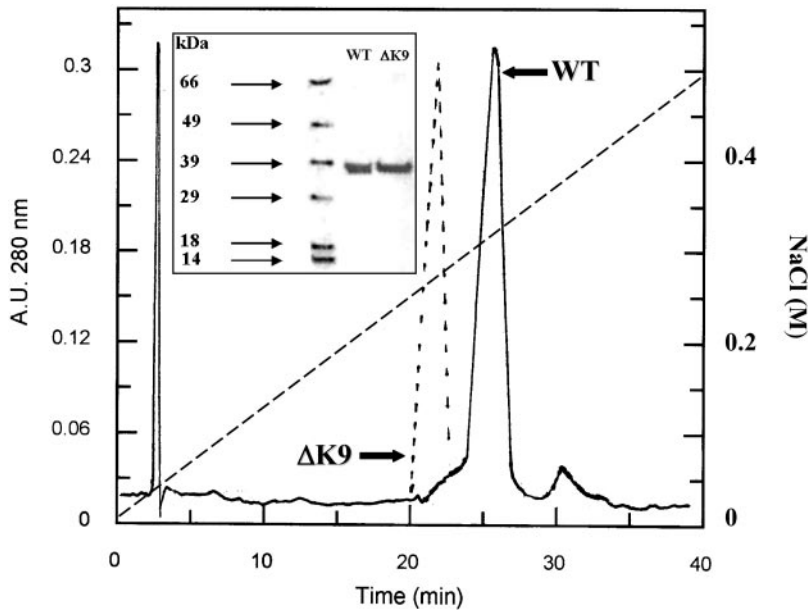

FIG. 1. **Ion exchange HPLC chromatograms of both activated WT (*solid line*) and ΔK9 mutant thrombin (*dashed line*).** The applied NaCl concentration gradient is shown on the *second* (*right*) *y* axis of the graph. In the *inset*, SDS-PAGE of purified WT and ΔK9 mutant thrombin under reducing conditions is also shown. The molecular weight markers were composed of bovine serum albumin (66 kDa), fumarase (49 kDa), alcohol dehydrogenase (39 kDa), carbonic anidrase (29 kDa), β-lactoglobulin (18 kDa), and α-lactalbumin (14 kDa).

the gas constant and T is the absolute temperature. The difference between the ΔG_c pertaining to the WT and the mutant form (*i.e.* $\Delta\Delta G_c = {}^{WT}\Delta G_c - {}^{m}\Delta G_c$) expresses the energetic contribution of the deleted lysine residue to the stabilization of the fast form. Based on our experimental data, a $\Delta\Delta G_c$ of −0.65 kcal/mol was calculated, which significantly provided evidence that the allosteric coupling between Na^+ binding and the stabilization of the enzyme in its more active form is reduced by the lysine deletion. This would suggest that Lys^9 deletion in the light chain should confer a "slow-like" conformation to the thrombin mutant. As further evidence of this behavior, using tosyl-Gly-Pro-Arg-*p*NA (Sigma) as substrate and thrombin in the fast forms, at 25 °C and pH 8.00, K_m values were equal to 3.62 ± 0.40 μM and 5.50 ± 0.60 μM for ΔK9 and WT thrombins, respectively, whereas k_{cat} values were 9.34 ± 1.50 and 101 ± 2.50 s^{-1} for ΔK9 and WT thrombins, respectively. The above data suggest that possible conformational variations induced in the active site by the deletion of Lys^9 may affect the intermediate steps of catalysis rather than substrate binding, which was proved to be even slightly favored in the mutant compared with the WT enzyme.

The viscosity perturbation experiments showed that the ΔK9 mutant has a slightly better interaction with the synthetic substrate D-Phe-Pip-Arg-*p*NA, by virtue of both a moderate increase of the association rate constant and decrease of the dissociation rate value (Table I). These experiments also showed that the hydrolytic cycle undergoes a strong decrease of the acylation step and that that Phe-Pip-Arg-*p*NA does not act as a "sticky" substrate for the mutant thrombin, at variance with what was observed for the WT form. As a matter of fact, the k_2/k_{-1} ratio was equal to about 0.02 and 0.5 for ΔK9 and WT forms, respectively (Table I).

Fibrinopeptide A Release

The hydrolysis of the Aα-chain from fibrinogen is markedly reduced in the ΔK9 mutant thrombin (Fig. 2). This effect is mostly due to a drastic change of the k_{cat} value, which decreases from 45.3 ± 2 s^{-1} in the WT to 1.82 ± 0.1 s^{-1} in the mutant form. The K_m parameter also changed, its value being equal to 5.1 ± 0.6 μM in the WT and 13 ± 2 μM in the ΔK9 mutant form (Table II).

TABLE I
Best fit values to Scheme 1 of catalytic and binding constants pertaining to WT and ΔK9 mutant thrombins (Phe-Pip-Arg-pNA as the substrate)

Enzymes	k_{+1}	k_{-1}	k_2	k_3	k_2/k_{-1}	K_d
	$\times 10^{-8}$ M^{-1} s^{-1}	s^{-1}	s^{-1}	s^{-1}		μM
WT	0.89 ± 0.02	180 ± 90	92 ± 5	1650 ± 1000	0.5	2.02
ΔK9	1.00 ± 0.20	120 ± 19	2.7 ± 0.2	20 ± 2	0.02	1.20

Protein C Activation and Interaction with Thrombomodulin

Hydrolysis of zymogen protein C by the ΔK9 thrombin form in the absence of thrombomodulin could not be followed under the experimental conditions used in this study, since the rate of protein C cleavage was too severely impaired to be monitored. In the presence of 100 nM thrombomodulin, the k_{cat}/K_m value was about 30-fold lower in the mutant thrombin (Table II), such an effect not depending upon an impairment of thrombomodulin interaction, as solid phase binding experiments proved. The K_d values of thrombomodulin binding were indeed very close in the two thrombin forms (Table II).

Interaction with PAR1 and GpIbα and Activation of Gel-filtered Platelets

The ΔK9 thrombin was defective in activating gel-filtered platelets, the EC_{50} value being equal to 38.6 ± 6 nM in the mutant and 2.1 ± 0.3 in WT form. In order to investigate the main causes of this impaired function, we studied the *in vitro* hydrolysis of the PAR1 38–60 peptide. This peptide bears both the sequence with the thrombin cleavage site and the domain interacting with the fibrinogen recognition exosite of the enzyme. In solution, this substrate showed a severe defect in interacting with ΔK9, largely due to a decrease of the k_{cat} value, as reported in Table II. The k_{cat}/K_m value decreased 116 times from 1.74×10^7 M^{-1} s^{-1} in WT to 1.5×10^5 M^{-1} s^{-1} in the mutant form, which corresponds at 25 °C to a net decrease of 2.8 kcal/mol in the activation free energy calculated on the basis of the ratio between the k_{cat} and K_m values.

The interaction with immobilized GpIbα was substantially unaffected by the mutation, the K_d values being similar in the two forms (Table II). Thus, the defective platelet activating

capacity of the mutant thrombin was mostly attributed to an impaired PAR1 interaction.

Interaction with Physiological and Synthetic Inhibitors

The best fit second order rate constants for both WT and ΔK9 thrombin interaction with AT in the presence and absence of heparin are listed in Table III. Under both conditions, AT interaction with the mutant thrombin decreased about 20 times, compared with the WT form. Such a defective interaction, not depending upon the heparin effect, suggests an impairment of the processes leading to the formation of the stable thrombin-AT complex.

Inhibition experiments under steady state conditions showed that the interaction of the ΔK9 thrombin with α-NAPAP was facilitated, the measured K_i value being equal to 0.66 ± 0.03 nM *versus* 2.1 ± 0.2 nM of the WT form (Table III). Likewise, BPTI binding was facilitated in the ΔK9 form, the measured K_d value decreasing about 3 times compared with the K_d value determined with the WT form.

All of the above functional studies showed that the catalytic machinery of thrombin is negatively affected by the loss of Lys^9 in the A-chain, suggesting that conformational changes occurring in the light chain may propagate to the active site cleft of the enzyme. This was a partly unexpected result, due to some contrasting findings reported in the literature about the influence of the A-chain on the catalytic activity of the human thrombin (11, 12). In fact, some authors provided evidence of a positive effect of the A-chain on the catalytic function of the human thrombin (12), whereas another group showed that the elimination of the A-chain in the bovine thrombin caused a nil effect (11).

Molecular Modeling of the Mutant Thrombin

Global Properties—In this study, we performed an MD simulation of a virtually generated ΔK9 mutant three-dimensional model and compared its key geometrical and conformational properties with available crystal structure data of WT enzyme forms. The goal was to detect structural properties possibly related to the observed different functional properties. As the starting model we used the x-ray structure of human thrombin covalently bound to D-Phe-Pro-Arg-methyl ketone determined at 1.9-Å resolution (Protein Data Bank entry 1PPB) (8). The inhibitor was removed, and the structure of the free enzyme was used to generate the mutant protein (Swiss-Prot; available on the World Wide Web at www.expasy.ch). The ΔK9 thrombin model was then allowed to evolve in fully explicit water solvent, using the MD protocol described in detail under "Experimental Procedures." Recently reported MD simulations performed by De Filippis *et al.* (31) with WT thrombin, using a protocol similar to that adopted by us, had shown that after about 5 ns, the protein undergoes a conformational transition from a more open conformation, proposed to be related to the fast form, to a more compact conformation, proposed to be related to the slow form. Decrease of the protein surface exposed to water and reduction of the radius of gyration (R_g, defined as the mass-weighted root mean square distance of a collection of atoms from their common center of mass) after 5-ns simulation had been brought as proofs of a more compact structure of the slow form with respect to the more active (fast) form. This model is in good agreement with the recent x-ray crystallographic studies by Huntington and Esmon (32), revealing a more "open" overall conformation of the fast form compared with the slow

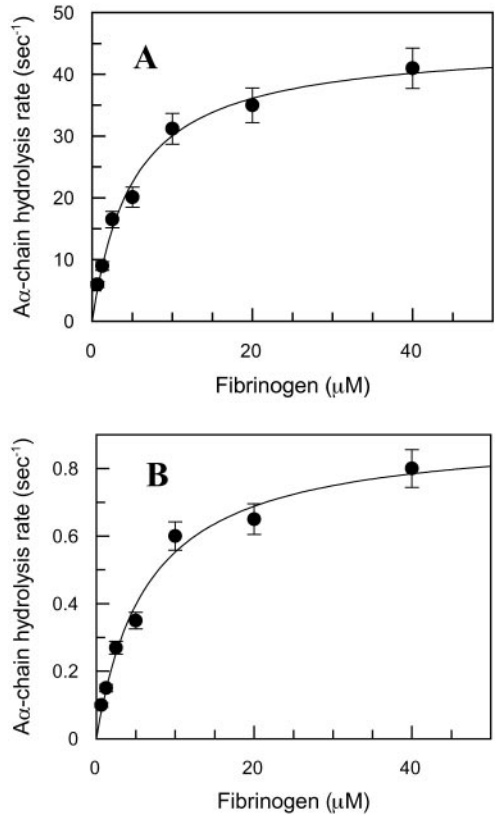

FIG. 2. **Measurement of steady-state kinetic parameters concerning fibrinopeptide A hydrolysis by WT (*A*) and ΔK9 mutant (*B*) thrombin.** *Continuous lines* were drawn according to the best fit k_{cat} and K_m values listed in Table II.

TABLE II
Best fit values catalytic and binding constants pertaining interaction with substrates and cell membrane receptors

Enzymes	FpA hydrolysis		Protein C hydrolysis	Thrombomodulin binding (K_d)	PAR1P hydrolysis		GpIbα binding (K_d)
	k_{cat}	K_m	(k_{cat}/K_m)		k_{cat}	K_m	
	s^{-1}	μM	$\times 10^{-6}\ M^{-1}\ s^{-1}$	nM	s^{-1}	μM	μM
WT	45.3 ± 2.0	5.1 ± 0.6	2.4 ± 0.2	2.14 ± 0.40	146 ± 6	8.4 ± 1.0	0.12 ± 0.02
ΔK9	1.82 ± 0.10	13 ± 2	0.07 ± 0.01	2.67 ± 0.30	4.2 ± 0.5	28 ± 7	0.13 ± 0.02

TABLE III
Kinetic parameters pertaining to inhibition of WT and ΔK9 mutant thrombin by ATIII, BPTI, and α-NAPAP

Enzymes	ATIII inhibition		BPTI binding (K_d)	α-NAPAP inhibition (K_i)
	k_{on}, H[a] = 0	k_{on}, H = 75 nM		
	$M^{-1}\ s^{-1}$		μM	nM
WT	$1.3 \pm 0.3 \times 10^4$	$6.8 \pm 0.8 \times 10^7$	109 ± 13	2.1 ± 0.2
ΔK9	$0.7 \pm 0.1 \times 10^3$	$0.30 \pm 0.06 \times 10^7$	40 ± 5	0.66 ± 0.03

[a] H, high molecular weight heparin.

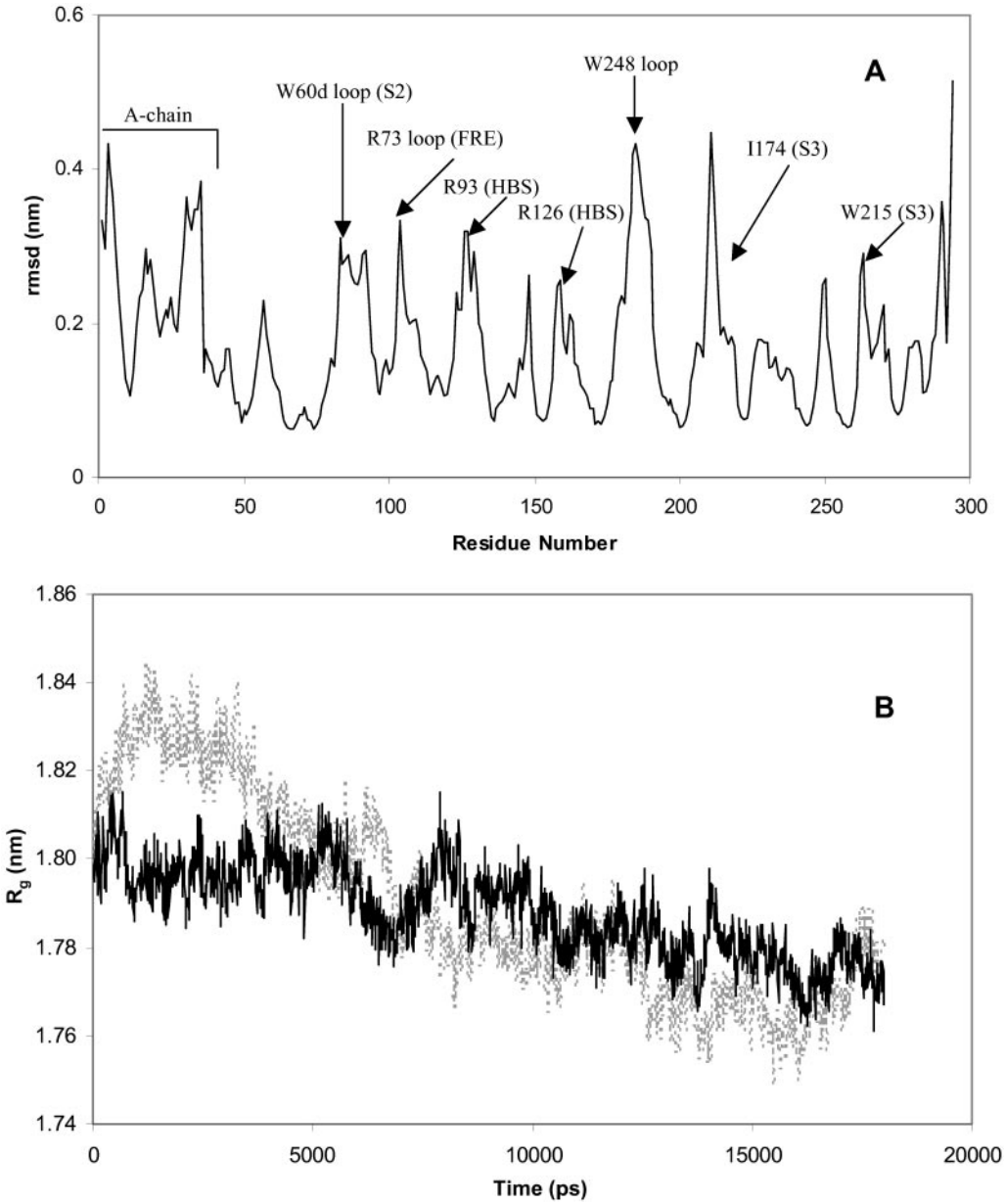

FIG. 3. *A*, root mean square fluctuation of backbone atoms of ΔK9 mutant thrombin during the MD simulation, with respect to the starting structure. The most flexible loops and residues in some relevant recognition binding sites, such as S2 and S3 (forming the so-called "aryl binding sites"), fibrinogen recognition exosite (*FRE*), and heparin binding site (*HBS*) are highlighted. *B*, variation of R_g (radius of gyration) of ΔK9 mutant (*solid line*) and WT thrombin (*dotted line*) as a function of time.

form of thrombin. Our MD computational approach, preliminarily applied to the study of the WT thrombin, reproduced a behavior quite similar to that reported in literature (31). Interestingly, the same MD simulation protocol applied to the ΔK9 mutant showed both similar and dissimilar behaviors. The mutant protein structure equilibrates with the potential energy of the system after about 5 ns. The root mean square deviation from the starting structure reaches a plateau value of 0.40 ± 0.05 nm between 5 and 18 ns. The overall secondary structure elements are in general stable along the whole trajectory (less than 1% of the secondary structures, mainly α-helices, were lost or varied during the production dynamics). The analysis of root mean square deviation fluctuation during the simulation for each atom position in the backbone (Fig. 3*A*), with respect to the starting structure, revealed the residues in the A-chain, the Trp^{148} loop (residues 180–190), and the Trp^{60d} loop (S2 subsite) as well as Arg^{93} and Arg^{126} of the heparin binding site, and the fibrinogen recognition exosite (Arg^{73} loop) as those having the highest degree of flexibility (root mean square deviation >0.3 nm). Conformational motions involving residues within the S3 site (especially Trp^{215} and Ile^{174}) were also inferred from the plot in Fig. 3*A*. These conformational changes were exactly observed when MD simulation was performed on the virtual mutant with deletion of the Lys^{10} instead of Lys^{9} residues (data not shown), indicating that deleting Lys^{9} or Lys^{10} should result in proteins having similar MD behaviors.

From the point of view of the global properties, the plot displaying the variation of R_g as a function of time (Fig. 3*B*) was of particular diagnostic significance, indicating that the transition around 5 ns involves a smaller diminution of R_g (it ranges from an average value of 1.80 nm in the first 5-ns simulation to an average value of 1.78 nm in the last 13-ns simulation), compared with the WT form (R_g values range between 1.84 and 1.76 nm, respectively). A more compact conformation of the ΔK9 mutant protein along all of the simulation time, inferred from the plot in Fig. 3*B*, is consistent with our

experimental data. In fact, Na^+ was responsible for a 4.5-fold and a 13-fold increase of the k_{cat}/K_m value of Phe-Pip-Arg-*p*NA hydrolysis by the ΔK9 mutant and WT thrombin, respectively.

A-chain Conformation—Deleting Lys^9 resulted in a restructuring of the light chain, with an average increase of the contact surface area of 85 $Å^2$ (Fig. 4). This finding, which gains relevance by taking into account the deletion of one residue in the mutant light chain, should mainly depend upon the lack of contacts (ion pairs reinforced by hydrogen bonds), which instead stabilizes the light chain in the WT protein in a conformation having a smaller contact surface. An account of the relevant contacts within the A-chain and between the A- and B-chains was provided by monitoring the ionic interactions during the last 10-ns simulation of the ΔK9 mutant. These ionic bonds had been proved important in stabilizing the A-chain in WT thrombin in a boomerang-like conformation (8). The results reported in Table IV showed that only the distances of the contacts Lys^{14a}-Asp^{14}, Glu^{13}-Arg^{14d} (intrachain salt bridges) and Asp^{1a}-Arg^{206}, Glu^{14e}-Lys^{186d} (interchain salt bridges) were close to those reported to be optimal in the crystal structure (8), whereas the remaining ionic interactions appeared disfavored. Such a change in electrostatic contacts could be a major cause of the refolding of the A-chain in the ΔK9 mutant.

Changes in the Specificity Sites and Surface Loops—In order to detect whether and how much the deletion of Lys^9 and the subsequent change in folding of A-chain affected conformational change in molecular regions mainly responsible for functional properties, we investigated in detail the MD behavior of residues located in the specificity sites (S1, S2, and S3) and in insertion loops (Table V). According to x-ray structure data (8) and similar MD studies (31), our MD simulation showed that the Trp^{148} loop appears as a region of high mobility, whereas the conformation of the Na^+-binding site remained quite stable during the simulation (31).

Conformational changes of ΔK9 residues within the S2 pocket (Trp^{60d} loop) are highlighted in the root mean square deviation calculations for backbone atoms (Fig. 3*A*). Also, residues lining the S3 site, such as in particular Trp^{215} and Ile^{174}, are located in protein loops highly fluctuating during the production dynamics. An account of the geometrical and conformational transitions involving residues within the specificity sites (namely Asp^{189} in the S1 site, Trp^{60d} and Tyr^{60a} in the S2 site, and Trp^{215} in the S3 site) that could significantly affect substrate or inhibitor docking into the enzyme cleft was obtained by monitoring the relative position of their side chains during the simulation of the ΔK9 mutant form. Thus, measuring Asp^{189}-Trp^{60d} relative positions resulted in an average distance between the centers of masses of 22.4 ± 1.4 Å in ΔK9, which is longer than that measured in the x-ray structure WT thrombin (19.7 ± 0.6 Å). The difference in the relative position of the aromatic side chains within the S2 site was even more appreciable, the distance between Trp^{60d} and Tyr^{60a} being about 2 times longer in the mutant (8.2 ± 0.6 Å), during the last 10-ns simulation, than in the WT forms (4.8 ± 0.1 Å). We reputed this result of particular relevance, since such a longer distance was observed both in the first part (6.4 ± 1.2 Å during the first 5 ns) of the simulation, believed to be related to the fast form, and the second part (7.7 ± 1.2 Å during the last 13 ns) of the simulation, probably related to the slow form (31). This could mean that the opening of the S2 site should similarly affect binding and catalysis both in the fast and in the slow allosteric forms. Such a geometrical variation in the S2 site may be in agreement with the increased association rate constant of the synthetic substrates and the moderate but significant decrease of K_i value of the inhibitor α-NAPAP, possibly due to a better accommodation of the P2 moieties in the ligands into the corresponding S2 enzyme binding site (Tables I and III). The models of the complexes between the two thrombins and NAPAP (not shown) revealed that the most striking difference between x-ray WT thrombin structures and

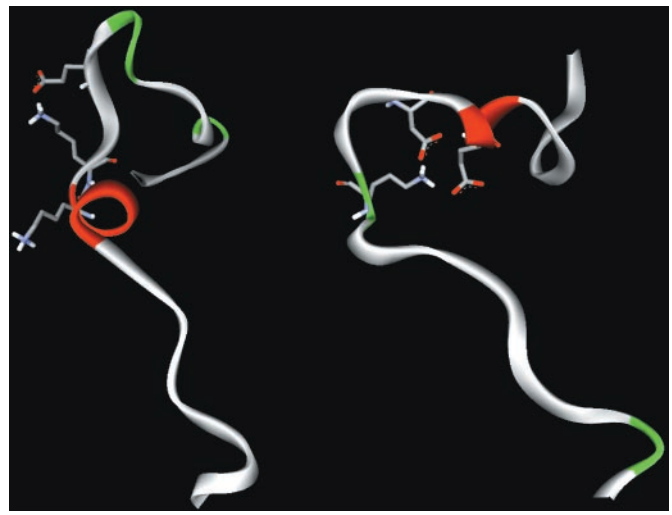

FIG. 4. **Three-dimensional structures of the A-chain in the lowest energy conformers of the WT form (*left side*) and ΔK9 thrombin mutant (*right side*).** *Red*, α-helix; *green*, turn. Displayed residue side chains are as follows: Lys^9, contacting Glu^{13} and Lys^{10} (WT); Lys^{10}, contacting Asp^{14} and Glu^{14c} (ΔK9).

TABLE IV
Ion pairs stabilizing A-chain and A-B interchain interactions in the ΔK9 mutant thrombin during the simulation
Shown are average distances ± S.D. for the last 10-ns simulation.

Ion clusters and salt bridges[a]	Average distance
	Å
Ion pairs stabilizing A-chain	
Lys^{14a}-Asp^{14} (6.0/5.3)	8.07 ± 0.45
Asp^{14}-Arg^4 (3.7/2.9)	3.28 ± 0.53
Arg^4-Glu^8 (4.2/2.1)	7.52 ± 1.04
Glu^{13}-Arg^{14d} (4.4/3.3)	5.95 ± 2.01
Ion pairs stabilizing interactions between A and B chains	
Asp^{1a}-Arg^{206} (6.0/4.2)	4.85 ± 1.42
Glu^8-Lys^{202} (3.8/2.8)	15.44 ± 2.01
Lys^{202}-Glu^{14c} (2.9/2.7)	7.91 ± 1.83
Asp^{14}-Arg^{137} (2.8/2.8)	6.19 ± 0.49
Lys^{135}-Glu^{14e} (3.8/2.8)	7.93 ± 1.55
Glu^{14e}-Lys^{186d} (4.0/3.6)	5.57 ± 1.32
Lys^{14a}-Glu^{23} (4.5/3.6)	8.24 ± 1.84

[a] Optimal distances between interacting groups in parentheses are taken from Ref. 6.

TABLE V
Average values obtained from MD simulation of ΔK9 mutant compared with crystal structure data of WT thrombins

Measurements	ΔK9	WT[a]
	Å	*Å*
S1, S2 and S3 binding sites[b]		
S1 (Asp^{189})-S2 (Trp^{60d})	22.5 ± 1.4	19.7 ± 0.6
S2 (Trp^{60d})-S2 (Tyr^{60a})	8.2 ± 0.1	4.8 ± 0.1
S2 (Trp^{60d})-S3 (Trp^{215})	14.0 ± 1.8	13.6 ± 0.3
S3 (Trp^{215})-S1 (Asp^{189})	9.6 ± 0.8	11.4 ± 0.3
Catalytic triad		
Ser^{195}-$O^{\gamma[\rho]}$–His^{57}-$N^{\epsilon[\rho]}$	2.96 ± 0.66	3.12 ± 0.40
Ser^{195}-$O^{\gamma[\rho]}$–His^{57}-$N^{\epsilon[\rho]}$ (angle, degrees)	109 ± 14°	86 ± 11°
Asp^{102}-$O^{\gamma 1}$–His^{57}-ND	8.27 ± 1.91	2.77 ± 0.13
Asp^{102}-$O^{\gamma 2}$–His^{57}-ND	8.11 ± 1.88	3.47 ± 0.15

[a] Average values calculated from the available Protein Data Bank crystal structures (n = 26, <1.9-Å resolution).
[b] Distance (Å) between centers of mass.

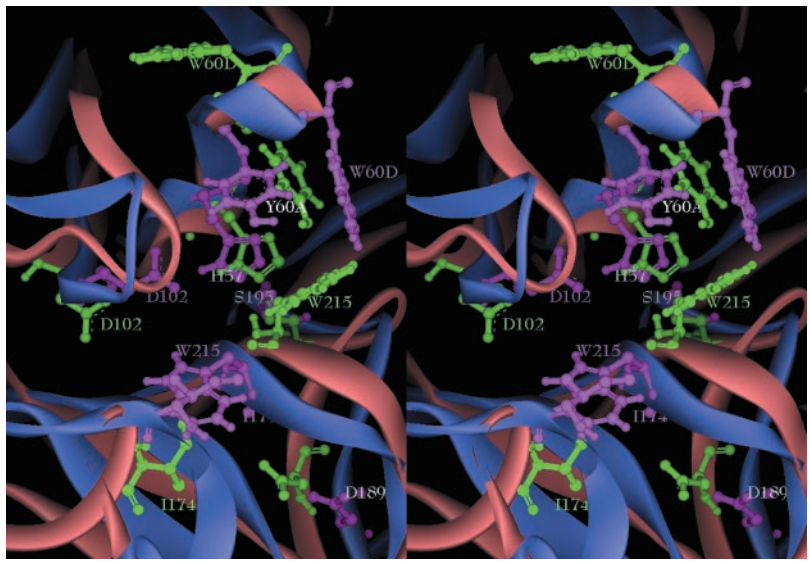

FIG. 5. **Stereoview of ribbon representation of the lowest energy structure of the ΔK9 mutant and the x-ray structure of the WT thrombin (Protein Data Bank 1PPB) aligned with GROMACS by using the "g_confirms" option (*blue*, ΔK9 mutant; *red*, WT thrombin).** Residues in the catalytic triad (Ser^{195}, His^{57}, and Asp^{102}) and in the S1 (Asp^{189}), S2 (Trp^{60d} and Tyr^{60a}) and S3 (Trp^{215} and Ile^{174}) binding sites are shown in *ball and stick* representation (*green*, ΔK9 mutant; *magenta*, WT thrombin).

ΔK9 mutant model pertains 1) to the S2 site, which rests as a lid on the active site of WT but not the mutant and 2) to Trp^{215} belonging to the S3 site, which is strongly shifted apart. It is noteworthy that the MD simulation revealing the expulsion/rearrangement of the S2 pocket and the global enlargement of the so-called "aryl binding site" in the mutated enzyme is consistent with the experimental finding that BPTI affinity increased roughly 3 times in the ΔK9 form (Table III). Although this is not a dramatic effect, previous studies showed that the Trp^{60d} loop is a major element opposing to the formation of thrombin-BPTI interaction, whereas its expulsion/rearrangement is able to increase the inhibitor's affinity for the enzyme (33). This arrangement should enhance the "capture radius" of the catalytic site, based on Hill's terminology (34), optimizing the complementarity of the inhibitor (or substrate) with the enzyme in the resting state. However, the steady-state measurements of this study indicated that the conformational transitions caused by the mutation/deletion reduce the complementarity of the substrate's binding to the enzyme's transition state, reducing the k_{cat}/K_m value. This effect is largely due to a drastic decrease of the acylation rate (Table I). However, although acylation remains the rate-limiting step of the catalytic cycle, both the acylation and deacylation reactions are similarly affected by the mutation (Table I). It is known that the acylation proceeds with Ser^{195}-O^{γ} as the nucleophile species attacking the carbonyl carbon of the scissile bond to form the acyl-enzyme. Deacylation reaction also involves a nucleophile attack with a water molecule as the incipient nucleophile. It is widely believed that in the two steps the $N^{\epsilon 2}$ of His^{57} imidazole acts as a general base catalyst, abstracting a proton from Ser^{195}-O^{γ} and water, respectively, and that the protonated imidazolium acts as a general acid catalyst donating a proton to the scissile peptide nitrogen or Ser^{195}-O^{γ} (30). It is thus conceivable that the mutation in ΔK9 thrombin may induce a shift in the pK_a values of the His^{57} imidazole group, altering both the acylation and deacylation step. Further experiments are in progress to address this issue.

Catalytic Triad Geometry—As far as the catalytic pocket is concerned, the geometries of the catalytic triad amino acids Asp^{102}, His^{57}, and Ser^{195} pertaining to 26 high resolution (<1.9-Å) thrombin crystal structures (one free, the others inhibitor-bound) were compared with the average distances and angles calculated in the MD frames of the last 10-ns simulation. Based on the findings of Huber *et al.* (35), assuming rotational freedom of the hydrogen atom around the Ser^{195} CB–OG bond, a Ser^{195}-CB-O^{γ}–His^{57}-N^{ϵ} angle of ~111° for a linear hydrogen bond should be expected. As can be seen in Table V, a hydrogen bond should be present between Ser^{195} and His^{57}, whereas the hydrogen bonds between Asp^{102} and His^{57}, present only in the first few ns of the simulation, are loss in the last 10-ns simulation, when the ΔK9 undergoes a conformational transition triggered by the restructuring of the A-chain folding. A careful look at the enzyme clefts shows a clear geometrical distortion of the active site in the model of ΔK9 mutant generated in this study compared with the crystal structure of a WT form taken as reference (Fig. 5). In the three-dimensional structure of WT thrombin, the side chain centroids of the amino acids Asp^{189} (S1), Trp^{60d} (S2), and Trp^{215} (S3) and the amino acids of the catalytic triad seem to lie on nearly parallel planes, whereas in the lowest energy model of the ΔK9 mutant, the two planes are quasiorthogonal. The distortion of the relative positions of the above amino acids into the catalytic pocket of the ΔK9 mutant may be hypothesized to be a major cause for the drastic decrease of the specificity constants measured with both synthetic and physiological substrates. Taken together, our results provided a computational support to the observation that Lys^{9} deletion could affect, through long range allosteric effects, the active site conformation. The latter should fit well established geometrical constraints (bond lengths and angles) in order to increase the nucleophilicity of the Ser^{195}-O^{γ} and a given relative geometry involving Ser^{195}-O^{γ} and amide carbonyl C of the substrates. An optimal distance between the Ser^{195}-O^{γ} and the carbonyl C and the pyramidalization at the carbonyl C allow the tetrahedral intermediate to be efficiently formed, according to the Bürgi-Dunitz-Shefter relation for nucleophile-electrophile interaction (35, 36).

Conclusions

A detailed understanding of the intramolecular mechanisms responsible for the functional defects observed in the ΔK9 mutant deserves further experimental and computational studies. Nevertheless, the results obtained from MD simulation reported herein allowed us to identify conformational changes that, starting from a restructuring of the A-chain folding, are transmitted to key molecular regions within the catalytic pocket, through a "domino-like" effect. It must be pointed out that, when present in other serine proteases, such as tissue plasminogen activator or urokinase, a noncatalytic A-chain disulfide-bonded to the active B-chain seems to play allosteric

roles for the involved enzyme (37). On the basis of the present findings, a similar conclusion can be hypothesized for the thrombin A-chain as well.

Our MD analysis highlighted the modification within the "aryl binding site," especially the expulsion/rearrangement of the Trp^{60d} side chain (S2 site) and the shifting of Trp^{215} (S3) and geometrical distortion within the catalytic triad as the possible main determinants of the decrease of ΔK9 catalytic activity.

Very recently, it has been shown that in serine proteases, evolutionarily conserved sparse networks of amino acid interactions represent the structural machinery by which the allosteric communication can take place, so that chemical signals originating at one site in an enzyme molecule may reliably propagate to distant functional sites (38). Two main networks of linked groups were identified, although the detailed mechanisms generating allosteric coupling are still unclear (38). Our results seem in agreement with those findings, indicating that critical A-chain residues could also participate to the allosteric linkage with the network around the S1 catalytic site, involving some surface loops, such as the 60-loop (38).

Finally, the evidence that the structural and conformational state of the A-chain can affect the catalytic activity of thrombin may have implications in the field of antithrombotic agent pharmacology. The recent development of peptides that bind to surface loops of coagulation factor VIIa, selectively inhibiting the enzyme activity (39), shows how stabilization of the "inactive" forms of this serine protease by exosite ligands can strongly affect enzyme function. Further studies are needed to show whether this could be a valuable approach for the modulation of thrombin activity.

Acknowledgment—R. D. C. is grateful to Dr. V. De Filippis (University of Padova) for valuable comments and suggestions.

REFERENCES

1. Akhavan, S., Mannucci, P. M., Lak, M., Mancuso, G., Mazzucconi, M. G., Rocino, A., Jenkins, P. V. & Perkins, S. J. (2000) *Thromb. Haemost.* **84,** 989–997
2. Sun, W. Y., Witte, D. P., Degen, J. L., Colbert, M. C., Burkart, M. C., Holmback, K., Xiao, Q., Bugge, T. H. & Degen, S. J. (1998) *Proc. Natl. Acad. Sci. U. S. A.* **95,** 7597–7602
3. Xue, J., Wu, Q., Westfield, L. A., Tuley, E. A., Lu, D., Zhang, Q., Shim, K., Zheng, X. & Sadler, J. E. (1998) *Proc. Natl. Acad. Sci. U. S. A.* **95,** 7603–7607
4. Lefkowitz, J. B., Haver, T., Clarke, S., Jacobson, L., Weller, A., Nuss, R., Manco-Johnson, M. & Hathaway, W. E. (2000) *Br. J. Haematol.* **108,** 182–187
5. Sun, W. Y., Smirnow, D., Jenkins, M. L. & Degen, S. J. (2001) *Thromb. Haemost.* **85,** 651–654
6. Akhavan, S., Luciani, M., Lavoretano, S. & Mannucci, P. M. (2003) *Br. J. Haematol.* **120,** 142–144
7. Ortiz, I., Lefkowitz, J., Weller, A. & Santiago-Borrero, P. (2002) *Haemophilia* **8,** 836 (abstr.)
8. Bode, W., Turk, D. & Karshikov, A. (1992) *Protein Sci.* **1,** 426–471
9. Hartley, B. S. (1970) *Phil. Trans. R. Soc. London Ser. B.* **257,** 77–87
10. Fujikawa, K., Legaz, M. E., Kato, H. & Davie, E. W. (1974) *Biochemistry* **13,** 4508–4516
11. Hageman, T. C., Endres, G. F. & Scheraga, H. A. (1975) *Arch. Biochem. Biophys.* **171,** 327–336
12. Sereiskaia, A. A., Osadchuk, T. V., Korneliuk, A. I., Pekhnik, I. V. & Serebrianyi, S. B. (1989) *Biokhimiia* **54,** 542–548
13. Akhavan, S., De Cristofaro, R., Peyvandi, F., Lavoretano, S., Landolfi, R. & Mannucci, P. M. (2002) *Blood* **100,** 1347–1353
14. Speijer, H., Govers-Riemslag, J. W., Zwaal, R. F. & Rosing, J. (1986) *J. Biol. Chem.* **261,** 13258–13267
15. Degen, S. J. & Davie, E. W. (1987) *Biochemistry* **26,** 6165–6177
16. De Cristofaro, R., Rocca, B., Bizzi, B. & Landolfi, R. (1993) *Biochem. J.* **289,** 475–480
17. Stone, S. R., Betz, A. & Hofsteenge J. (1991) *Biochemistry* **30,** 9841–9848
18. Wells, C. M. & Di Cera, E. (1992) *Biochemistry* **31,** 11721–11730
19. De Cristofaro, R. & Landolfi, R. (1994) *J. Mol. Biol.* **239,** 569–577
20. Picozzi, M., Landolfi, R. & De Cristofaro, R. (1994) *Eur. J. Biochem.* **219,** 1013–1021
21. De Cristofaro, R. & Landolfi, R. (1999) *Eur. J. Biochem.* **260,** 97–102
22. De Cristofaro, R., De Candia E., Rutella, S. & Weitz, J. I. (2000) *J. Biol. Chem.* **275,** 3887–3895
23. Berendsen, H. J. C., Postma, J. P. M., van Gunsteren, W. F., Di Nola, A. & Haak, J. R. (1984) *J. Chem. Phys.* **81,** 3684–3690
24. van Gunsteren, W. F., Daura, X. & Mark, A. E. (1998) *Encycl. Comput. Chem.* **2,** 1211–1216
25. Berendsen, H. J. C., Postma, J. P. M., van Gunsteren, W. F. & Hermans, J. (1981) in *Intermolecular Forces* (Pullman, B., ed) pp. 331–342, Reidel, Dordrecht, The Netherlands
26. Hess, B., Bekker, H., Fraaije, J. & Berendsen, H. J. C. (1997) *J. Comput. Chem.* **18,** 1463–1472
27. Fischer, B. E., Schlokatm, U., Mittererm, A., Grillbergerm, L., Reiterm, M., Mundtm, W., Dorner, F. & Eibl, J. (1996) *Protein Eng.* **9,** 921–926
28. Petrovan, R. J., Govers-Riemslag, J. W., Nowa, G., Hemker, H. C., Tans, G. & Rosing, J. (1998) *Biochemistry* **37,** 1185–1191
29. Di Cera, E., Guinto, E. R., Vindigni, A., Dang, Q. D., Ayala, Y. M., Wuyi, M. & Tulinsky, A. (1995) *J. Biol. Chem.* **270,** 22089–22092
30. Fersht, A. (1985) *Enzyme Structure and Mechanism*, pp. 405–411, W. H. Freeman & Co., New York
31. De Filippis, V., Colombo, G., Russo, I., Spadari, B. & Fontana, A. (2002) *Biochemistry* **41,** 13556–13569
32. Huntington, J. A. & Esmon, C. T. (2003) *Structure* **11,** 469–479
33. van de Locht, A., Bode, W., Huber, R., Le Bonniec, B. F., Stone, S. R., Esmon, C. T. & Stubbs, M. T. (1997) *EMBO J.* **16,** 2977–2984
34. Hill, T. L. (1975) *Proc. Natl. Acad. Sci. U. S. A.* **72,** 4918–4922
35. Marquart, M., Walter, J, Deisenhofer, J., Bode, W. & Huber, R. (1983) *Acta Crystallogr. Sec. B* **39,** 480–490
36. Bürgi, H. B., Dunitz, J. D. & Shefter, E. (1973) *J. Am. Chem. Soc.* **95,** 5065–5067
37. Geppert, A. G. & Binder, B. R. (1992) *Arch. Biochem. Biophys.* **297,** 205–212
38. Süel, G. M., Lockless, S. W., Wall, M. A. & Ranganathan, R. (2003) *Nat. Struct. Biol.* **10,** 59–69
39. Dennis, M. S., Eigenbrot, C., Skelton, N. J., Ultsch, M. H., Santell, L., Dwyer, M. A., O'Connell, M. P. & Lazarus, R. A. (2000) *Nature* **404,** 465–470 .

A Natural Prothrombin Mutant Reveals an Unexpected Influence of A-chain Structure on the Activity of Human α-Thrombin

Raimondo De Cristofaro, Sepideh Akhavan, Cosimo Altomare, Andrea Carotti, Flora Peyvandi and Pier Mannuccio Mannucci

J. Biol. Chem. 2004, 279:13035-13043.
doi: 10.1074/jbc.M312430200 originally published online January 13, 2004
